Jurnal Teknologi

Full Paper

THE INFLUENCE OF THE NON-SYMMETRIC PUNCHING PROCESS PARAMETER ON THE HOLE SHAPE AND QUALITY OF A COMMERCIALLY PURE TITANIUM SHEET

Muslim Mahardika[a,b], Yani Kurniawan[c*], Suyitno[a,b], Muhammad Haritsah Amrullah[d], Budi Arifvianto[a,b]

[a]Department of Mechanical and Industrial Engineering, Faculty of Engineering, Universitas Gadjah Mada, 55281, Indonesia
[b]Centre for Innovation of Medical Equipments and Devices/CIMEDs, Department of Mechanical and Industrial Engineering, Faculty of Engineering, Universitas Gadjah Mada, Indonesia
[c]Department of Mechanical Engineering, Faculty of Engineering, Pancasila University, Jakarta, Indonesia
[d]Department of Mechanical Engineering, Politeknik Manufaktur Negeri Bangka Belitung, Indonesia

Article history
Received
7 April 2021
Received in revised form
13 August 2023
Accepted
6 September 2023
Published Online
20 December 2023

*Corresponding author
yani.kurniawan@univpancasila.ac.id

Graphical abstract

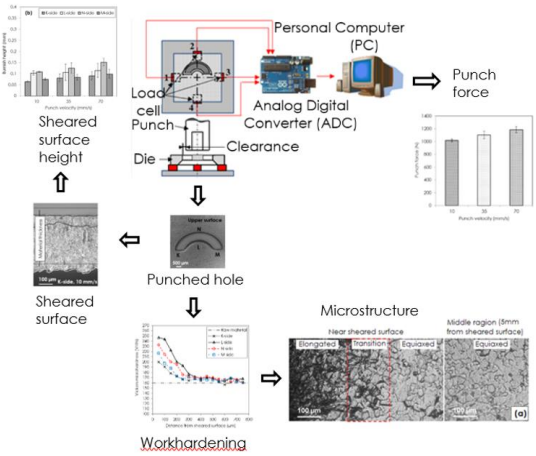

Abstract

Recently, punching technology has become one of the promising manufacturing techniques for a thin metallic sheet. The processing parameters used in this technique have been recognized to influence the hole shape produced in the working materials. Therefore, it is important to understand the effect of the punching process parameters on the hole shape and quality over the manufactured materials. This study aims to determine the influence of the punching process on the non-symmetrical hole shape and quality over a commercially pure titanium sheet. The effect of punch speed on the punch force and the sheared surface is also studied, by applying the punch velocities of 10, 35 and 70 mm/s. The sheared surface of the hole was examined at its four different sides, namely K (straight), L (outer radius), N (inner radius) and M (straight). The results show uneven distribution of punch strength as detected at the affected region of the non-symmetrical hole. In addition, the punch force increased with the increase of punch speed. Meanwhile, the sheared surfaces on each side were apparently different. The burnish height on the side of the radius was found to be about 0.038 mm higher than that on the straight side. The burnish height on the radius side increases by 0.43 mm with the increasing punch speed from 10 to 70 mm/s. However, the increased punch velocity did not always increase the burr height. The work hardening that occurs on the straight side is smaller by about 15% than the radius side.

Keywords: Non-symmetric punching, punching process, punch force, sheared surface, work hardening

1.0 INTRODUCTION

Titanium and its alloys have been widely used as biomedical implant materials owing to its excellent biocompatibility and corrosion resistance [1-4]. Femoral stems, artificial knee joints, artificial lumbar discs, bone scaffolds, and osteosynthesis plates are among some examples of biomedical implants that have been successfully made from this material. Furthermore, a number of fabrication techniques have been performed for preparing such metallic implants, such as casting [2, 5-6], machining, forming [7], and electric discharge machining [8].

Wire electrical discharge machining (WEDM) and electrical discharge machining (EDM) are the non-conventional machining processes [9], in which no direct contact occurs between the tool and the workpiece [8, 10], and therefore it can avoid deformation over a thin workpiece [9]. With this machining technique, the material removal occurs due to melting temperature; therefore WEDM and EDM require an electric current greater than 1A [8, 10-13]. Material removal rate requires a long time; in WEDM, it is about 8.29 mm^3/min with current of 120 A and 17.9 µs pulse duration [11], while in EDM, it is about 27 mg/min when using current of 10A with pulse duration of 50 µs [13]. Not only that, the workpiece after machining with WEDM and EDM will form a white layer (or a recast layer) on the surface [11-13]. This layer has benefits in terms of increased abrasion and erosion resistance, but also defects in it, such as cavities, cracks, or induced stresses which cause overall damage to mechanical component properties [10], [13]. Surface cracking defects may cause a reduction in material resistance to fatigue and corrosion [14], especially under tensile load conditions [15]

This shows that the WEDM and EDM process in fabricated plate type implants still requires an additional process to increase the material resistance against fatigue and corrosion, especially under tensile load conditions, as well as a large current to speed up the machining process. Additional processes and large current cause the price of WEDM and EDM products to be expensive. Another alternative to overcome this problem is the forming process, which has several advantages, such as good surface quality, high accuracy and good efficiency at a concurrent high quantity [16]. To achieve these advantages, the forming process must consider the parameters used. This is because the process parameters have different effects on different materials and shapes. The forming process consists of several processes, namely drawing (or stamping), blanking, and punching. Studies on these processes include research on the effect of process parameters on various materials and product shapes. Deep drawing process parameters has been studied by Dwivedi and Agnihotri [17]. The effect of holder pressure and size on the rectangular micro deep drawing has been investigated by Aminzahed *et al*. [18], whereas evaluation of micro deep drawing has been carried out by soft die-simulation and experiments by Irthiea and Green [19]. The finite element and extended strain-based forming limit diagram can be used for predicting the forming severity [20]. Moreover, the finite element method also was used for studying the influence of several process parameters in blanking. The effect of clearance and punch velocity on the quality of blank parts has been investigated in copper [21] and brass [22]. An innovative technique for reducing die-roll size during the fine-blanking process was studied by Luo *et al*. using a simulation and experiment method [23]. In addition, Canales *et al*. investigated sheet metal blanking process by numerical simulation [24]. A novel modified die design for fine-blanking process to reduce the die-roll size was investigated by Liu *et al*. [25]. Sahli *et al*. investigated the effect of clearance on the forming quality in the fine blanking process using finite element simulation and experiment [26]. Meanwhile, wear-induced edge passivation of fine-blanking punches was been investigated by Zheng *et al*. [27]. In punching processes, the effect of process parameters was studied on various shapes of holes, including circular, triangular, hexagonal, and non-symmetric holes.

The effect of process parameter was studied on circular punching, concerning the punch velocity, clearance, punch wear, etc. The effect of punch velocity has been investigated in brass, steel, copper, and aluminum. The effect of punch velocity in brass is indicated by increased punch velocity (from 5 to 50 mm/s) increased burnish height by 32%, and decreased value of surface roughness (Ra) from 0.105 to 0.040 µm [28]. In steel, it is discovered that the increased punch velocity increases the punch force [29], whereas in copper, the increased punch velocity does not necessarily increase the hardness of the punched hole's upper surface [30]. However, in aluminum, work hardening when using low velocity is higher than that when using high velocity [31].

Furthermore, the effect of clearance is also investigated in brass, bronze, aluminum and steel. In brass, the burnish height increases along with the decreasing clearance [28], [32] while a simulation analysis by Kwak *et al*. [33] in steel also shows the same result. According to Xu *et al*. [28] the optimal clearance is 5% of thickness, resulting in the burnish height of 130 µm with burnish height ratio of 80% when using punch velocity of 1 mm/s. On the other hand, according to Kibe *et al*. [32] a clearance of 5% with punch velocity of 1 mm/s results in the burnish height ratio of 50% on bronze, 78% on brass, and 75% on aluminum.

The effect of punch wear was studied on steel, brass and titanium. In brass, Luo [34] observed the wear condition of the tool and the punch hole surface on the brass. Enhancing sheared surfaces was performed by Xu *et al*. [35] by increasing the quality of punch surfaces with ion beam irradiation. This study also was carried out on steel [36]. On titanium, the study of punch wear effect on the punched holes' quality was conducted by Guo and Tam [36]. In addition, the effect of carbon nanotubes coating on

punch wear was investigated by Guo and Tam [37]. The effect of processing time on the finishing of micro holes has been studied, as well [38].

Triangular and hexagonal punching was studied by Chern and Wang [39] in copper. It found that the burr height decreased with decreased clearance, as the burr height resulted was shorter when using clearance of 5%. Moreover, non-symmetric punching was investigated by Subramanian *et al*. [40] in steel. This investigation shows that the sheared surface quality in each edge is different as evident by the higher burnish height in radius edge than that in the straight edge.

Based on the literature review, studies on the punching process in titanium are mostly done on the circular shape or focus on punch wear. In addition, non-symmetric punching process in titanium has not been investigated. In order to develop the punching process in the manufacture of implants, it is necessary to investigate non-circular shapes. This is because the implant fabrication in the punching process requires various shapes, not just the circular one. Therefore, the research aimed to investigate the non-symmetric punching process in titanium. The effect of velocity on punch force, sheared surface and workhardening was also investigated.

2.0 METHODOLOGY

Non-symmetric shape is based on one of the punching processes in manufacturing medical equipment, namely the straight plate type implants. Schematic illustration of the punching process can be seen in Figure 1, while the non-symmetric shape dimension is shown in Figure 2. The testing material used was commercially pure titanium with a thickness of 400 µm and hardness of 160 VHN. A pneumatic punch machine was used for testing with punch velocities of 10, 35 and 70 mm/s. The punch material used was high-speed steel (HSS) SKH9, with punch-die clearance of 30 µm.

The punch force is measured using four Zemic L6E load-cells (Zemic Europe B.V., Netherlands) which are placed under die as shown in Figure 1. The capacity of each loadcell used was 500 N. Meanwhile, the punched holes were investigated at four different positions, namely K-side (straight), L-side (outer radius), N-side (inner radius) and M-side (straight), as seen in Figure 3. To aid in the analysis of the punched holes, the sheared surfaces of the punched hole were examined visually and measured by using a Dino-lite AM2111 optical microscope (Anmo, Taiwan). To aid in the analysis of all the quantitative data obtained in this research, a statistical analysis was carried out by using two-factor with replication ANOVA. Analysis of variance (ANOVA) is used to determine the contribution of each factor while identifying significant factors or their interactions. The work-hardening phenomenon over the sheared subsurface of the Ti plate was determined by using Vickers microhardness test (Buehler, USA) with an indentation load of 0.98 N which was held for 10 s during the indentation (ASTM E384). The microhardness measurement was conducted at the location as indicated in Figure 4. The microstructure of the Ti sheet was characterized by using optical microscope (Olympus, Japan) after a series of preparation steps for metallographic analysis by using 20% HCl, 40% HF, and 40% H_2O. The microstructure observation was conducted at the location as indicated in Figure 5.

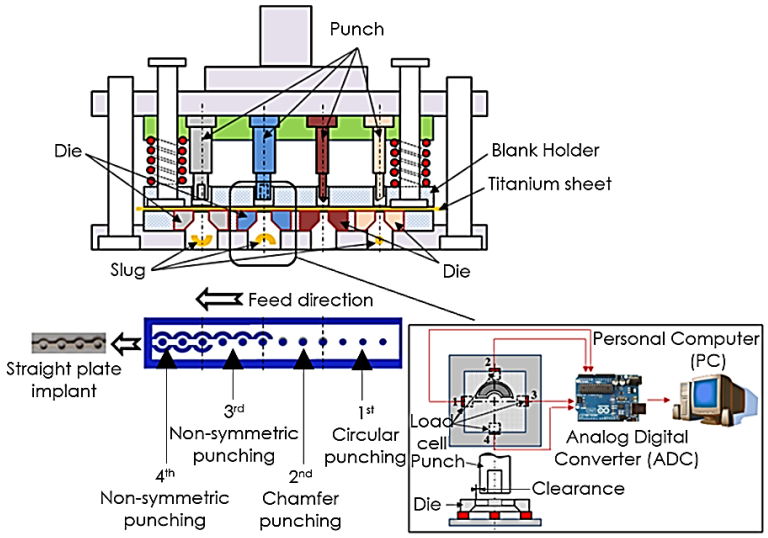

Figure 1 Schematic illustration of the punching process

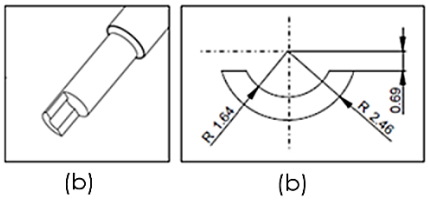

Figure 2 (a) The shape and (b) geometry of the punch used in this research

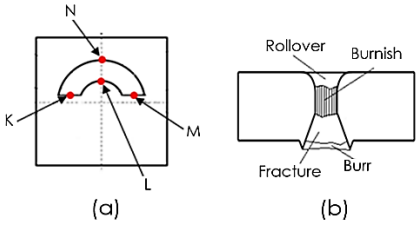

Figure 3 (a) Position of measurement and (b) shape of sheared surface

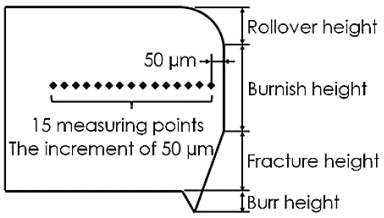

Figure 4 Position of microhardness measurement

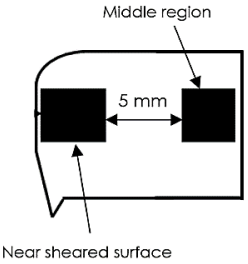

Figure 5 Location of microstructure observation

3.0 RESULTS AND DISCUSSION

3.1 Punched Force

The result of the punch force measurement from the experiment employing three different punch velocities is shown in Figure 6. Figure 6(a) shows the punch force average observed during the experiment. This figure shows that a punch velocity of 70 mm/s has a bigger punch force, and a punch velocity of 10 mm/s has the smallest punch force. Figure 6(b) shows the punch force distribution in different loadcell positions. This figure shows that the punch force in loadcell position 2 is the biggest, and loadcell position 4 is the smallest.

The results of the ANOVA statistical test presented in Table 1 shows that the P_{value} is lower than 0.05, and the F is higher than F_{crit} for punch velocity and loadcell position. It indicates that there are significant data differences from the punch force measurement results of the changes in the punch velocity and loadcell position. Therefore, it can be concluded that the punch force can be affected by punch velocity and loadcell position. In this case, the punch force increases along with the increasing punch velocity, and the punch force distribution is affected when the loadcell position is different.

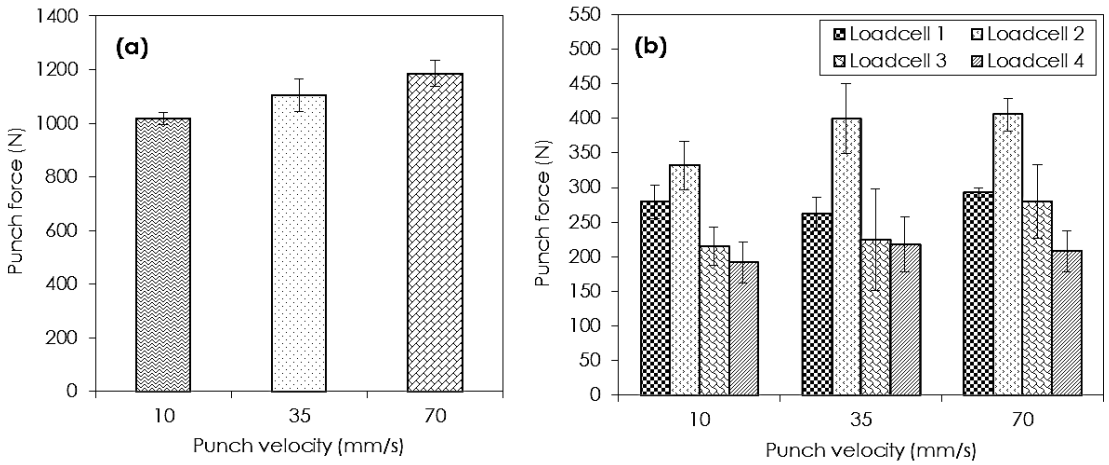

Figure 6 Punch force: (a) total force and (b) force in each load cell

In the punching process using a punch velocity of 35 mm/s, the punch force increases by 8% compared to that if using a punch velocity of 10 mm/s. Additionally, the punch force increases by about 17% when the punching process uses a punch velocity of 70 mm/s. This result shows that the punch force increases along with the increasing punch velocity. This is because the increase of velocity causes the increasing change of momentum rate in the punch movement. Based on Newton's second law of motion, the rate of change of momentum of an object is equal to the net force applied [41]. Therefore, punch velocity increases along with the increase of the punch force. This result has a similar trend as findings from previous studies [42-44]. Moreover, the investigation conducted by Larue *et al*. also found that the punch force is directly proportional to the momentum rate [29], in which the force is directly proportional to mass and velocity, while it is inversely proportional to cutting time. When the punch speed increases, the cutting time decreases, and the cutting force also increases.

Table 1 Analysis of variance for punch force

Source of Variation	SS	df	MS	F	P_{value}	F_{crit}
Punch velocity	20897.52	2	10448.76	5.62	0.01	3.19
Loadcell position	240443.38	3	80147.79	43.07	1.17E-13	2.80
Interaction	13776.47	6	2296.08	1.23	0.31	2.29
Error	89318.92	48	1860.81			
Total	364436.28	59				

Note: SS is sum of squares, df is stand for degrees of freedom, MS is mean square, F is ratios of mean squares, P_{value} is probability or significance value, F_{crit} is critical ratios of mean squares

The punch force distribution is different in each loadcell as shown in Figure 6(b). It shows the punch force at the 2nd load cell position was bigger with 73%, 83%, and 95% than that at the 4th load cell position when the punching process uses punch velocities of 10, 35, and 70 mm/s respectively. This difference of the punch force is because the 2nd load cell position is near the center of force on the non-symmetric shape, while the 4th load cell position is far from the center of force. Based on the force equilibrium [45], when the support distance is closer to the force center, the force received by the support is greater. Conversely, when the support distance is farther from the force center, the force received by the support is smaller. This is the reason of why the force in the 2nd load cell position is bigger than that the 4th load cell position.

3.2 Punched Holes

The observation results over the upper and lower surface of the punched holes are shown in Figure 7. The upper surface shows that the shape of the cutting edge on the K and M sides look almost the same as the edge shape. Side N looks sharp, while L side is blunt. The underside, the burr, is formed in all sides.

Figure 8 show a series of the macrographs depicting the sheared surfaces of the holes with punch velocity of 10, 35 and 70 mm/s, respectively. As seen in these figures, there are four regions in the sheared surfaces of the punched holes, namely the rollover zone (Ro), burnish zone (Brns), fracture zone (Fr), and burr zone (Br), as identified from the upper side to the lower side of the plate.

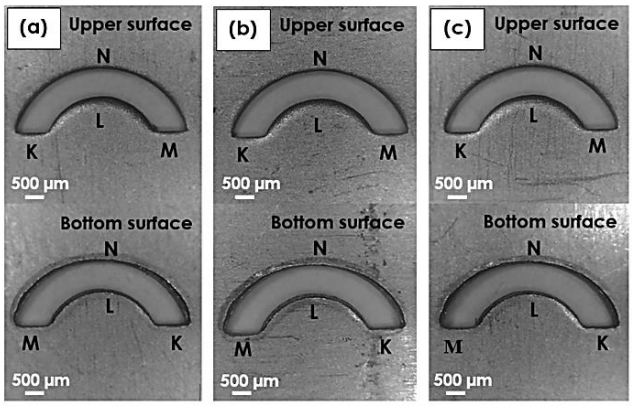

Figure 7 Shape of upper and lower surface of the punched holes: (a) 10 mm/s, (b) 35 mm/s, and (d) 70 mm/s

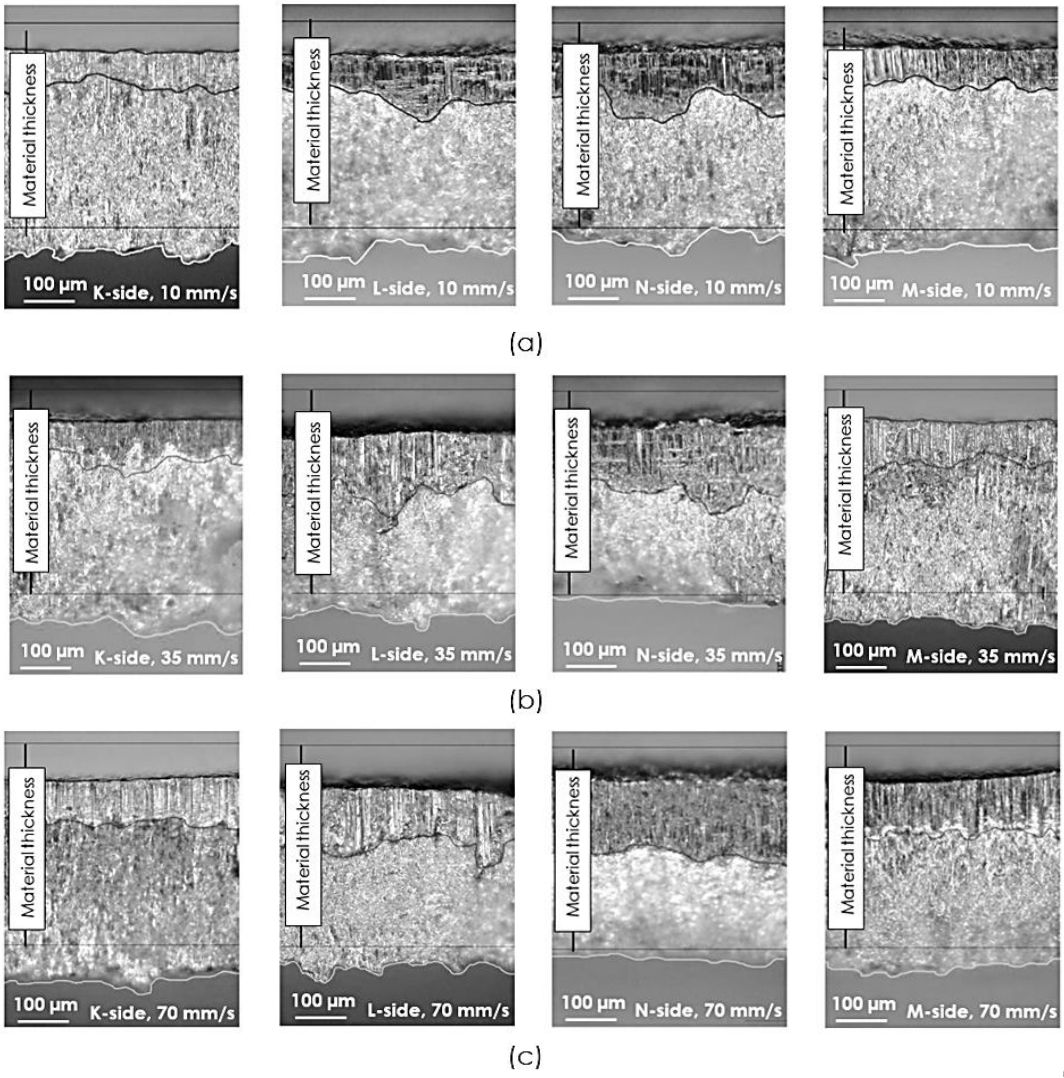

Figure 8 Macrographs of sheared surfaces with punch velocity: (a) 10 mm/s, (b) 35 mm/s, and (c) 70 mm/s

The illustration of the burr formation from the rollover is shown in Figure 9. Rollover is a region at the top of the cut surface. This corresponds to the depression made by the punch in the work prior to cutting. It is the region where the initial plastic deformation occurs in the work. Just below the rollover is a relatively smooth region called the burnish. This results from penetration of the punch into the work

before fracture begins. Beneath the burnish is the fractured zone, a relatively rough surface of the cut edge where continued downward movement of the punch causes the fracture of the metal. Finally, at the bottom of the edge is a burr, a sharp corner on the edge caused by elongation of the metal during the final separation of the two pieces. As shown in Figure 8, the morphologies of the sheared surfaces are apparently the same.

The measurement results of the sheared surface height with punch velocities of 10, 35, and 70 mm/s are presented in Figure 10. As seen in this figure, the average value of the sheared surface height in all sides appears to have the same trend when the punching process uses punch velocities of 10, 35, and 70 mm/s. At punch velocity of 70 mm/s, the heights of the rollover, burnish, and burr resulted is the highest. Meanwhile, the heights of the rollover, burnish, and burr resulted when using a punch velocity of 10 mm/s is the shortest. Rollover height on the straight side (K-side and M-side) is higher than that on the N-side (inner radius). However, it is shorter than that on the L-side (outer radius). Burnish height on the radius side (N-side and L-side) is higher than that on the straight side (K-side and M-side), and the burr height on the straight side is higher than that on the radius side. This result has the same trend as prior research [40].

The results of the ANOVA statistical test of punch velocity and position (side shape) on the sheared surface is presented in Table 2. The analysis result of rollover, burnish and fracture show that the P_{value} is less than 0.05 and F is greater than F_{crit} in both parameters. This can be interpreted that there is a significant difference from the results of the rollover, burnish and fracture heights with changes of punch velocity and position (side shape). Meanwhile, the result of analysis on the burr shows that there is no significant influence of the punch speed on the height of this region. This indicated by P_{value} greater than 0.05 and F smaller than F_{crit}. However, there is a significant difference in the changes of position (side shape), as shown by the P_{value} smaller than 0.05 and F greater than F_{crit}. From these results, it can be concluded that the heights of the rollover, burnish, and fracture are affected by punch velocity and position (side shape), but the burr height is merely affected by position.

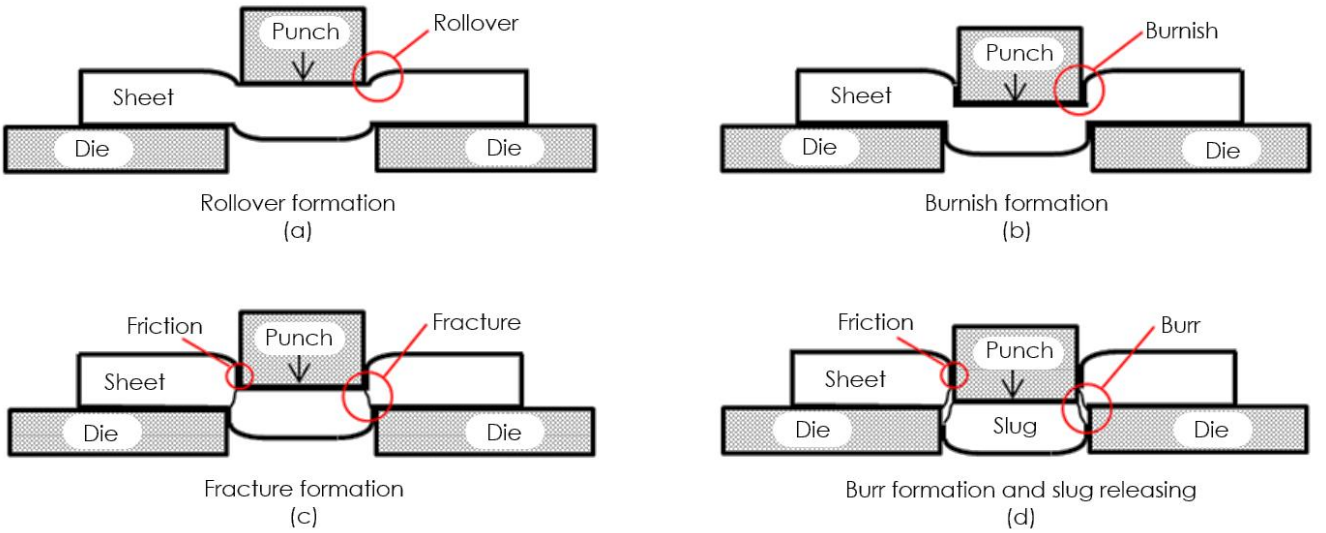

Figure 9 Step of punching process. (a) rollover formation, (b) burnish formation, (c) fracture formation, (d) burr formation and slug releasing

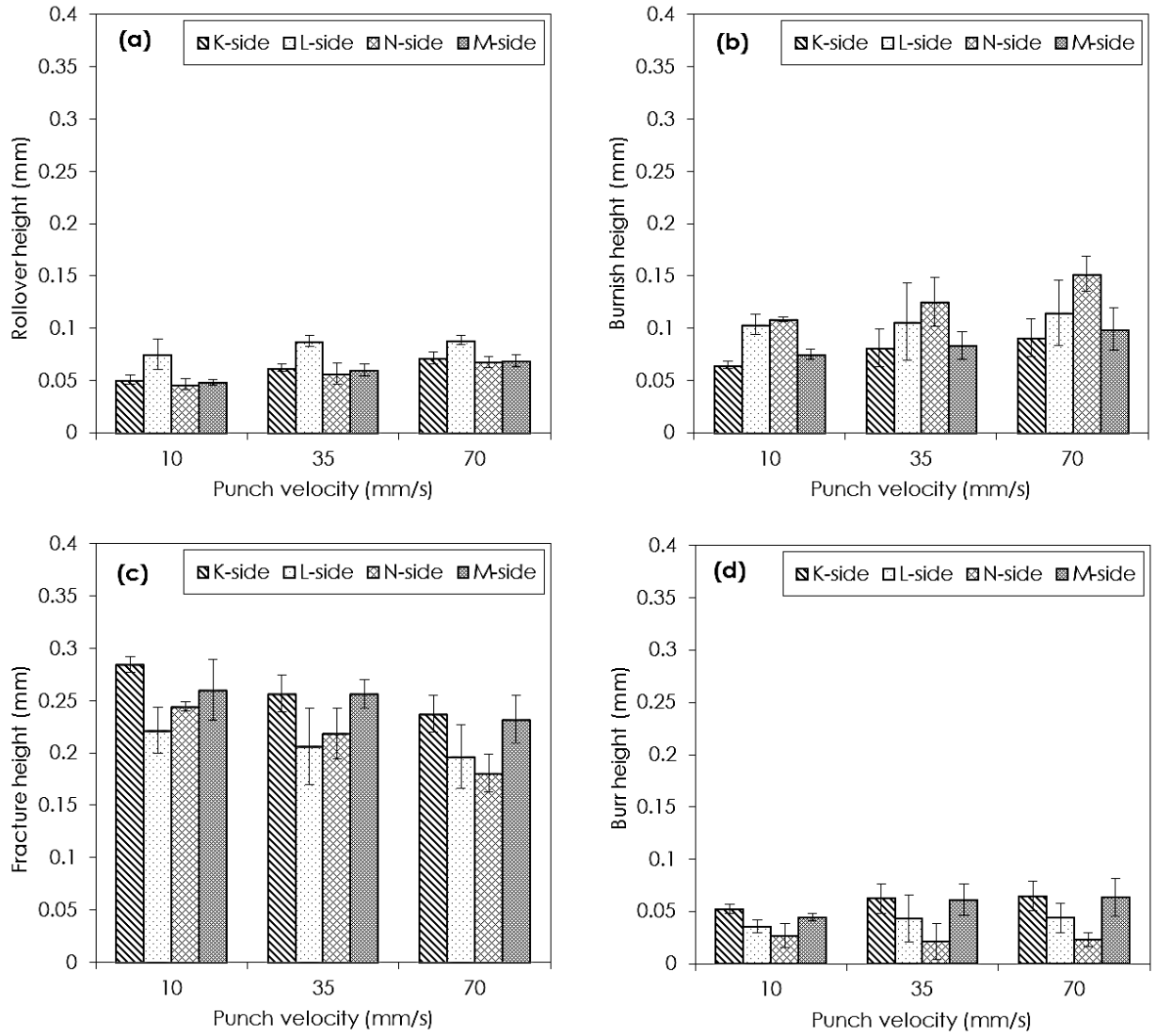

Figure 10 Measurement result of the sheared surfaces height in all side with a punch velocity varians: (a) rollover height, (b) burnish height, (c) fracture height, and (d) Burr height

The effect of punch velocity in the non-symmetric punching process is the increased rollover and burnish heights and decreased fracture height along with the increase of punch velocity. Rollover height (Figure 10 (a)) on the K-side when using punch velocities of 35 and 70 mm/s increases by 23% and 42% respectively compared to that with punch velocity of 10 mm/s. Rollover height on the L-side with the same punch velocities increases by 17% and 18%, respectively. On the N-side, rollover height increases by 23% and 47% when using punch velocities of 35 dan 70 mm/s, respectively. On the M-side with the same punch velocities, rollover height increases by 24% and 42%, respectively. Burnish height (Figure 10(b)) when using punch velocities of 35 and 70 mm/s on the K-side increases by 25% and 40% compared to that with a punch velocity of 10 mm/s. On the L-side with the same punch velocities, burnish height increases by 2% and 11%, respectively. On the N-side, burnish height increases by 15% and 40% when using punch velocities of 35 dan 70 mm/s respectively. On the M-side with the same punch velocities, burnish height increases by 11% and 32%, respectively. Increased burnish height will be followed by the decrease in fracture height (Figure 10(c)). Fracture height on the K-side when using punch velocities of 35 and 70 mm/s decreases by 10% and 17% respectively compared to that at punch velocity of 10 mm/s. Fracture height on the L-side with the same velocity decreases by 7% and 11%, respectively. On the N-side, the fracture height decreases by 11% and 26% when using punch velocities of 35 and 70 mm/s respectively. Fracture height on the M-side with the same velocities decreases by 1% and 11% respectively.

Table 2 Analysis of variance for sheared surface height

Source of Variation	SS	df	MS	F	P_{value}	F_{crit}
Rollover						
Punch velocity	0.002	2	0.0011	26.05	9.67E-07	3.40
Position	0.004	3	0.0014	32.13	1.43E-08	3.01
Interaction	0.000	6	1.70E-05	0.39	0.88	2.51
Error	0.001	24	4.33E-05			
Total	0.008	35				
Burnish						
Punch velocity	0.004	2	0.0020	58.76	5.66E-10	3.40
Position	0.014	3	0.0045	130.38	5.47E-15	3.01
Interaction	0.001	6	0.0001	4.12	0.01	2.51
Error	0.001	24	3.49E-05			
Total	0.019	35				
Fracture						
Punch velocity	0.010	2	0.0050	24.13	1.8E-06	3.40
Position	0.018	3	0.0058	27.99	5.22E-08	3.01
Interaction	0.002	6	0.0003	1.41	0.25216	2.51
Error	0.005	24	0.0002			
Total	0.034	35				
Burr						
Punch velocity	0.001	2	0.0003	2.89	0.08	3.40
Position	0.007	3	0.0025	26.84	7.67E-08	3.01
Interaction	0.001	6	8.60E-05	0.94	0.49	2.51
Error	0.002	24	9.17E-05			
Total	0.011	35				

Note: SS is sum of squares, df is stand for degrees of freedom, MS is mean square, F is ratios of mean squares, P_{value} is probability or significance value, F_{crit} is critical ratios of mean squares

This phenomenon of increased rollover and burnish heights occurs may be due to a slight increase in material elongation when there is a collision between punch and the material. Based on the conservation of energy and momentum in the collision, some of the kinetic energy is converted into heat energy when an inelastic collision occurs [41]. Moreover, in the punching process after the burnish formation, the punch still moves downwards until the burr is released as shown in Figure 9. The punch movement causes friction and creates heat in the burnish area. It is possible that such heat and friction were the factors which can increase the burnish height. Therefore, when the punch speed is high, the resulting burnish height is increased, as reported a previous study [43].

Position can affect the sheared surface height because the non-symmetric punching process has resulted in different grain movements on each position as shown in Figure 11. The straight side (K side and M side) has a unidirectional direction of grain movement, while on the inner radius side (N-side) the grain movement is centered on the radius. The grain movement centered on the radius has a higher compressive stress than the unidirectional direction of grain movement in the sheet along the deformation zone, as reported in previous studies [40]. This high compressive stress increases rollover height and delays the fracture set, hence increasing the burnish height. This causes the rollover height on the straight side (K-side and M-side) to be higher, and the burnish height to be shorter than that of the inner radius (N-side), whereas the height of the burr is higher than the inner radius (N-side) and outer (L-side). On the outer radius (L-side), grain movement spreads away from the center of the radius. The movement away from the center radius exerts a large tensile effect on the punching process, resulting in a higher rollover height than that on the inner radius and the straight edge. However, the burnish height is higher than that on the straight side and shorter than that on the inner radius side. The height of the burr is shorter than that on the straight side but higher than that on the inner radius side.

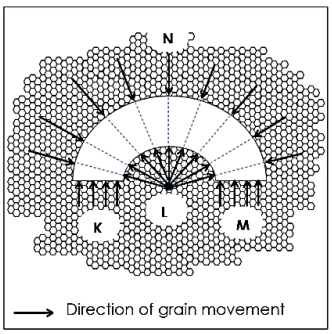

Figure 11 Direction of grain movement in a non-symmetric punching process

3.2 Workhardening

Work-hardening is a phenomenon that occurs following the plastic deformation of a ductile material. Similar to the mechanism in material cutting [46], plastic deformation is involved in the sequences of the machining process through micro-punching. Therefore, work-hardening may take place following the plastic deformation in the machining and punching process of titanium-based materials [44]. The effect of work-hardening could be seen from the increasing hardness and strength of a ductile material [30]. Therefore, the microhardness changes in the sheared surface of the punched hole need to be investigated to confirm the work-hardening that may occur during the micro-punching process of pure titanium sheet in this research.

Figure 12 show the micro hardness distributions in the sheared surface of the punched hole when using punching velocity of 70 mm/s. The non-symmetric punching process can increase the micro hardness on the sliding surface of the perforated holes. This has the same trend as that of the circular punching process [42-44]. However, in the non-symmetric punching process, it can be seen that the distribution of increased violence on each side looks different. The increase in hardness on the K-side is the smallest, while the largest increase in hardness occurs on the L-side. The increase in hardness on the N-side is greater than that of the K-side and M-side, but is smaller than that of the L-side. From these results, it can be concluded that the increase in hardness on the straight side (K-side and M-side) is smaller than the radius side (L-side and N-side).

This is due to differences in grain movement during the punching process as seen in Figure 11, which allows the plastic deformation that occurs on each side to be different, as well. The movement of grain in any direction results in greater plastic deformation than unidirectional grain movement. The greater plastic deformation can be characterized by the greater hardness value. It can be seen that the hardness value on the L-side increased to 23.5%, greater than that on the K-side, and 14% greater than that on the M-side. Meanwhile on the N-side, it is 16% bigger than the K-side and 7% bigger than the M-side.

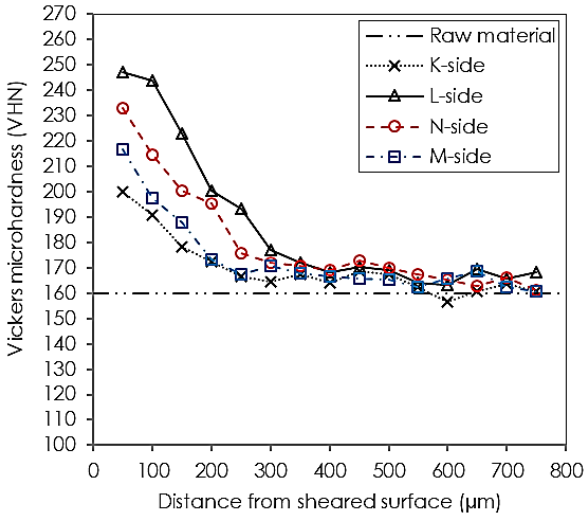

Figure 12 Micro hardness distributions in the sheared surface of the punched hole when using punching velocity of 70 mm/s

The result of this increase in hardening is also interesting to note as the hardness value obtained shows a dependence on the shape of the cut side around the non-symmetric hole. Numerous studies have also shown that cold working plastic deformation is the cause of increased hardening near the cut surface [31, 42, 44]. To confirm the work hardening phenomenon in the non-symmetric punching process, the microstructure test was carried out near the cut side of the burnish area on each side (K-side, L-side, N-side, and M-side) with a punch speed of 70 mm/s. Figure 13 shows the microstructure of the observations on each side. The microstructure images on the K, L, N and M sides show a change in grain structure from equiaxed to elongated. The change in grain from equiaxed to elongated causes the hardness value near the cutting side to be harder than the part far from the cutting side (700 µm distance) as shown in Figure 12. This occurs because the plastic deformation that occurs during the punching process causes changes in the structure of the grain, i.e. from equiaxed to elongated grain as confirmed in previous studies [40, 42].

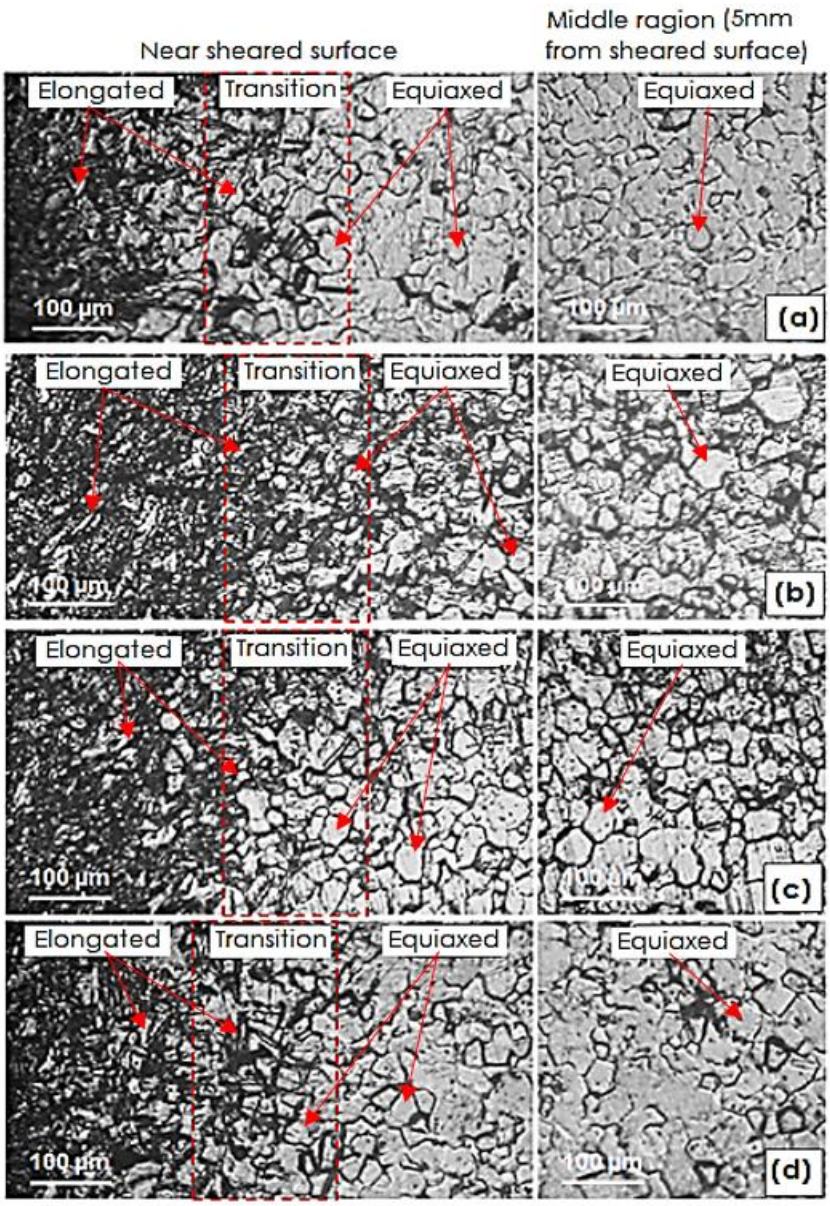

Figure 13 Micro structure in sheared surface: (a) K-sied, (b) L-side, (c) N-side, and (d) M-side

4.0 CONCLUSION

The non-symmetric punching process of the pure titanium sheet shows that the distribution of punch forces on each side is different. The greatest punching force is up to 406 N at loadcell 4. In addition, the punch force increases with increasing punch speed. The greatest punching force reaches 1186 N when using a punch speed of 70 mm/s.

The resulting sheared surface on each side is different, in which the heights of rollover and burnish on the side of the radius is higher than those on the straight side. Moreover, the rollover and burnish heights also increase with increased punch speed, whereas the burr height on the straight side is higher than that on the radius. However, the increased punch velocity does not always increase the burr height. The highest burnish (152 mm) is produced on the N-side when the punching process uses a punch speed of 70 mm/s.

The work hardening that occurs on each side is different, where the radius side (L-side and N-side) is greater than the straight side (K-side and M-side). The highest work hardening occurred on the L-side around 243 VHN, while the lowest work hardening occurred on the K-side around 191 VHN.

Conflicts of Interest

The author(s) declare(s) that there is no conflict of interest regarding the publication of this paper.

Acknowledgement

This research is fully supported by RTA-2020 grant (Rekognisi Tugas Akhir) Universitas Gadjah Mada, Indonesia.

References

[1] Van Noort, R. 1987. Titanium: The Implant Material of Today. *Journal of Materials Science*. 22(11): 3801-3811. Doi: https://doi.org/10.1007/BF01133326.

[2] Acero, J., Calderon, J., Salmeron, J. I., Verdaguer, J. J., Concejo, C., & Somacarrera, M. L. 1999. The Behaviour of Titanium as a Biomaterial: Microscopy Study of Plates and Surrounding Tissues in Facial Osteosynthesis. *Journal of Cranio-maxillofacial Surgery*. 27(2): 117-123. Doi: https://doi.org/10.1016/S1010-5182(99)80025-0.

[3] Arifvianto, B., Suyitno., & Mahardika, M. 2013. Surface Modification of Titanium using Steel Slag Ball and Shot Blasting Treatment for Biomedical Implant Applications. *International Journal of Minerals, Metallurgy, and Materials*. 20(8): 788-795. Doi: https://doi.org/10.1007/s12613-013-0797-1.

[4] Prayoga, B. T., Dharmastiti, R., Akbar, F., & Suyitno. 2018. Microstructural Characterization, Defect and Hardness of Titanium Femoral Knee Joint Produced using Vertical Centrifugal Investment Casting. *Journal of Mechanical Science Technology*. 32(1): 149-156. Doi: https://doi.org/10.1007/s12206-017-1216-8.

[5] Sutiyoko, Suyitno, Mahardika, M., & Syamsudin, A. 2016. Prediction of Shrinkage Porosity in Femoral Stem of Titanium Investment Casting. *Archives of Foundry Engineering*. 16(4): 157-162. Doi: 10.1515/afe-2016-0102.

[6] Setyana, L. D., Mahardika, M., Sutiyoko, S., & Suyitno, S. 2019. Influence of Gate Shape and Direction during Centrifugal Casting on Artificial Lumbar Disc Model of cp-ti. *Acta Metallurgica Slovaca*. 25(3): 193-202. Doi: http://dx.doi.org/10.12776/ams.v25i3.1315.

[7] Salim, U. A., Suyitno, Magetsari, R., & Mahardika, M. 2017. Development of the Gliding Hole of the Dynamics Compression Plate. *IOP Conference Series: Materials Science and Engineering*. 172(1): 012060. Doi: https://doi.org/10.1088/1757-899X/172/1/012060.

[8] Alias, A., Abdullah, B., & Abbas, N. M. 2012. Influence of Machine Feed Rate in wedm of Titanium Ti-6Al-4V with Constant Current (6A) using Brass Wire. *Procedia Engineering*. 41: 1806-1811. Doi: https://doi.org/10.1016/j.proeng.2012.07.387.

[9] Schey, J. A. 2000. *Introduction to Manufacturing Processes*. Third Edition. Mc Graw Hill Higher Education.

[10] Lee, H. T., & Tai, T. Y. 2003. Relationship between EDM Parameters and Surface Crack Formation. *Journal of Materials Processing Technology*. 142(3): 676-683. Doi: https://doi.org/10.1016/S0924-0136(03)00688-5.

[11] Kumar, A., Kumar, V., & Kumar, J. 2013. Experimental Investigation on Material Transfer Mechanism in WEDM of Pure Titanium (Grade-2). *Advances in Materials Science and Engineering*. Doi: http://dx.doi.org/10.1155/2013/847876.

[12] Kumar, A., Kumar, V., & Kumar, J. 2016. Surface Crack Density and Recast Layer Thickness Analysis in WEDM Process through Response Surface Methodology. *Machining Science and Technology*. 20(2): 201-230. Doi: http://dx.doi.org/10.1080/10910344.2016.1165835.

[13] Yan, B. H., Tsai, H. C., & Huang, F. Y. 2005. The Effect in EDM of a Dielectric of a Urea Solution in Water on Modifying the Surface of Titanium. *International Journal of Machine Tools and Manufacture*. 45(2): 194-200. Doi: https://doi.org/10.1016/j.ijmachtools.2004.07.006.

[14] Muthuramalingam, T., Mohan, B., & Jothilingam, A. 2014. Effect of Tool Electrode Resolidification on Surface Hardness in Electrical Discharge Machining. *Materials and Manufacturing Processes*. 29(11-12): 1374-1380. Doi: http://dx.doi.org/10.1080/10426914.2014.930956.

[15] Kumar, S., & Dhingra, A. K. 2018. Effects of Machining Parameters on Performance Characteristics of Powder Mixed EDM of Inconel-800. *International Journal of Automotive and Mechanical Engineering*. 15(2): 5221-5237. Doi: https://doi.org/10.15282/ijame.15.2.2018.6.0403.

[16] Newton, T. R., Melkote, S. N., Watkins, T. R., Trejo, R. M., & Reister, L. 2009. Investigation of the Effect of Pocess Parameters on the Formation and Characteristics of Recast Layer in Wire-EDM of Inconel 718. *Materials Science and Engineering A*. 513-514: 208-215. Doi: https://doi.org/10.1016/j.msea.2009.01.061.

[17] Lim, L. C., Lee, L. C., Wong, Y. S., & Lu, H. H. 1991. Solidification Microstructure of Discharge Machined Surfaces of Tool Steels. *Materials Science and Technology*. 7(3): 239-248. Doi: https://doi.org/10.1179/mst.1991.7.3.239.

[18] Ramulu, M., Jenkins, M. G., & Daigneault, J. A. 1997. Spark-Erosion Process Effects on the Properties and Performance of a TiB2 Particulatereinforced/sic Matrix Ceramic Composite. *Ceramic Engineering and Science Proceeding*. 18(3): 227-238. Doi: https://doi.org/10.1002/9780470294437.ch25.

[19] Thomson, P. F. 1989. Surface Damage in Electrodischarge Machining. *Materials Science and Technology*. 5(11): 1153-1157. Doi: https://doi.org/10.1179/mst.1989.5.11.1153.

[20] Eichenhueller, B., Egerer, E., & Engel, U. 2007. Microforming at Elevated Temperature - forming and Material Behavior. *The International Journal of Advanced Manufacturing Technology*. 33: 119-124. Doi: https://doi.org/10.1007/s00170-006-0731-z.

[21] Aminzahed, I., Mashhadi, M. M., & Sereshk, M. R. V. 2017. Investigation of Holder Pressure and Size Effects Inmicro Deep Drawing of Rectangular Work Pieces Driven by Piezoelectric Actuator. *Materials Science and Engineering C*. 71: 685-689. Doi: https://doi.org/10.1016/j.msec.2016.10.068.

[22] Irthiea, K., & Green, G. 2017. Evaluation of Micro Deep Drawing Technique using Soft Die-simulation and Experiments. *The International Journal of Advanced Manufacturing Technology*. 89(5-8): 2363-2374. Doi: https://doi.org/10.1007/s00170-016-9167-2.

[23] Shirin, M. B., Hashemi, R., & Assempour, A. 2018. Analysis of Deep Drawing Process to Predict the Forming Severity Considering Inverse Finite Element and Extended Strain-based Forming Limit Diagram. *Journal of Computational and Applied Research in Mechanical Engineering*. 8(1): 39-48. Doi: https://doi.org/10.22061/jcarme.2018.1750.1152.

[24] Lubis, D. Z., & Mahardika, M. 2016. Influence of Clearance and Punch Speed on the Quality of Pure Thin Copper Sheet Blanked Parts. *IOP Conference Series: Material Science Engineering*. 157(1): 012012:1-6. Doi: https://doi.org/10.1088/1757-899X/157/1/012012.

[25] Ristiawan, I., & Mahardika, M. 2017. Effect of Clearance and Punch Speed on the Cutting Surface Quality Results of a Brass Blanking on the Micropunch CNC Machine. *AIP Conference Proceedings*. 1831(1): 020054-1-020054-9. Doi: https://doi.org/10.1063/1.4981195.

[26] Xu, J., Guo, B., Shan, D., Wang, C., Li, J., Liu, Y., & Qu, D. 2012. Development of a Micro-forming System for Micro-punching Process of Micro-hole Arrays in Brass Foil. *Journal of Materials Processing Technology*. 212(11): 2238-2246. Doi: https://doi.org/10.1016/j.jmatprotec.2012.06.020.

[27] Larue, A., Ranc, N., Qu, Y. F., Millot, M., Lorong, P., & Lapujoulade, F. 2008. Experimental Study of a High Speed Punching Process. *International Journal of Material Forming*. 1(1): 1427-1430. Doi: https://doi.org/10.1007/s12289-008-0104-2.

[28] Meng, B., Fu, M. W., Fu, C. M., & Wang, J. L. 2015. Multivariable Analysis of Micro Shearing Process Customized for Progressive Forming of Micro-Parts. *International Journal of Mechanical Sciences*. 93: 191-203. Doi: https://doi.org/10.1016/j.ijmecsci.2015.01.017.
[29] Gotoh, M., & Yamashita, M. 2001. A Study of High-rate Shearing of Commercially Pure Aluminum Sheet. *Journal of Materials Processing Technology*. 110(3): 253-264. Doi: https://doi.org/10.1016/S0924-0136(00)00879-7.
[30] Kibe, Y., Okada, Y., & Mitsui, K. 2007. Machining Accuracy for Shearing Process of Thin-sheet Metals - Development of Initial Tool Position Adjustment System. *International Journal of Machine Tools and Manufacture*. 47(11): 1728-1737. Doi: https://doi.org/10.1016/j.ijmachtools.2006.12.006.
[31] Kwak, T. S., Kim, Y. J., & Bae, W. B. 2002. Finite Element Analysis on the Effect of Die Clearance on Shear Planes in Fine Blanking. *Journal of Materials Processing Technology*. 130-131: 462-468. Doi: https://doi.org/10.1016/S0924-0136(02)00767-7.
[32] Lou, S. Y. 1997. Studies on the Wear Conditions and the Sheared Edges in Punching. *Wear*. 208(1-2): 81-90. Doi: https://doi.org/10.1016/S0043-1648(96)07439-X.
[33] Xu, J., Guo, B., Shan, D., Wang, C., & Wang, Z. 2013. Surface Quality Improvements of WC–Co Micro-punch Finished by Ion Beam Irradiation for Micro-punching Process of Metal Foil. *Surface and Coatings Technology*. 235: 803-810. Doi: https://doi.org/10.1016/j.surfcoat.2013.06.114.
[34] Guo, W., & Tam, H. Y. 2012. Effects of Extended Punching on Wear of the WC/Co Micropunch and the Punched Microholes. *The International Journal of Advanced Manufacturing Technology*. 59(9-12): 955-960. Doi: https://doi.org/10.1007/s00170-011-3567-0.
[35] Guo, W., & Tam, H. Y. 2014. Effects of Carbon Nanotubes on Wear of WC/Co Micropunches. *The International Journal of Advanced Manufacturing Technology*. 72(1-4): 269-275. Doi: https://doi.org/10.1007/s00170-014-5661-6.
[36] Guo, W., & Tam, H. Y. 2013. Influence of the Processing Time on the Finishing of Punched Micro Holes by Planetary Stirring with Natural Sand Grains. *Journal of Engineering Manufacture*. 227(6): 1-9. Doi: https://doi.org/10.1177/0954405413476676.
[37] Chern, G. L., & Wang, S. D. 2007. Punching of Noncircular Micro-holes and Development of Micro-forming. *Precision Engineering*. 31(3): 210-217. Doi: https://doi.org/10.1016/j.precisioneng.2006.09.001.
[38] Subramonian, S., Altan, T., Ciocirlan, B., & Campbell, C. 2013. Optimum Selection of Variable Punch-die Clearance to Improve Tool Life in Blanking Non-symmetric Shapes. *International Journal of Machine Tools and Manufacture*. 75: 63-71. Doi: https://doi.org/10.1016/j.ijmachtools.2013.09.004.
[39] Giancoli, D. C. 2014. *Physics Principles with Applications*. 7th ed. Pearson Prentice Hall, Boston.
[40] Kurniawan, Y., Mahardika, M., Suyitno, Amrullah, M. H. 2019. Effect of Preheating on Punch Force, Sheared Surface and Work Hardening In Cold Punching Process of Commercially Pure Titanium Sheet. *International Review of Mechanical Engineering (IREME)*. 13(9): 504-512. Doi: https://doi.org/10.15866/ireme.v13i9.17398.
[41] Kurniawan, Y., Mahardika, M., & Suyitno. 2020. Effect of Punch Velocity on Punch Force and Burnish Height of Punched Holes in Punching Procces of Pure Titanium Sheet. *Journal of Physics: Conference Series*. 1430(012053): 1-7. Doi: https://iopscience.iop.org/article/10.1088/1742-6596/1430/1/012053.
[42] Kurniawan, Y., Mahardika, M., & Suyitno. 2020. The Effect of Punch Geometry on Punching Process in Titanium Sheet. *Jurnal Teknologi*. 82(2): 101-111. Doi: https://doi.org/10.11113/jt.v82.13947.
[43] Meriam, J. L., & Kraige, L. G. 2006. *Engineering Mechanics Statics.* 7th ed. John Wiley & Sons, United states of America.
[44] Groover, M. P. 2010. Fundamentals of *Modern Manufacturing: Materials, Processes, and Systems.* 4th ed. John Wiley & Sons, United States of America.